

High Frequency Acoustic Channel Characterization for Propagation and Ambient Noise

Martin Siderius
HLS Research Inc.
12730 High Bluff Drive, Suite 130, San Diego, CA 92130
Phone: (858) 755-9647 Fax: (858) 228-1734 Email: siderius@hlsresearch.com

Award Number: N00014-05-C-0116
<http://www.hlsresearch.com>

LONG-TERM GOALS

The long term goals of this project are to research the physics of high frequency (1-50 kHz) acoustic propagation and ambient noise in the ocean. This work is relevant to many types of Navy sonars such as active ASW and MCM systems and underwater acoustic modems for communications. Improved understanding is leading to better ways to adapt to and exploit the environment for enhanced system performance.

OBJECTIVES

One objective of this year's work has been to develop an accurate, dynamic acoustic model that could be used to understand observed Doppler spread in communications transmissions. The Doppler spread is caused by a combination of effects due to vertical and horizontal velocity components introduced through surface and source/receiver motion. A second objective for this year has been to develop a data inversion strategy for estimating geoacoustic properties of the seabed using the ambient noise field. Cross-correlation (Passive Fathometer) ambient noise processing [1] was applied with high resolution beamforming methods to better identify seabed layers. This was used to constrain the geoacoustic inversion for the properties of each seabed layer [2].

APPROACH

The approach for this work was to develop a modeling capability that captures the important Doppler spread of communications signals and compare this with data which was measured during the 2005 Makai experiment. To model Doppler spread at communications frequencies, Gaussian beam tracing was used. This provides an efficient capability to simulate broadband signals with a single ray/beam trace. Further, Gaussian beams are conveniently interpolated and extrapolated to allow for the treatment of Doppler effects due to environmental and/or source/receiver motion.

Experimental approach: Makai 2005

The Makai experiment took place from September 15 to October 2, 2005 near the coast of Kauai, HI. The site has a coral sand bottom with a fairly flat bathymetry that was nominally 100 m. The water column was variable but typically had a mixed layer depth of 40-60 m and was downward refracting below. The data was measured on September 24th using both stationary and towed sources (from R/V Kilo Moana). The sources were programmable research modems developed at SPAWAR Systems Center (referred to as the Telesonar Testbeds). Signals were received on the AOB2 array, an

Report Documentation Page

Form Approved
OMB No. 0704-0188

Public reporting burden for the collection of information is estimated to average 1 hour per response, including the time for reviewing instructions, searching existing data sources, gathering and maintaining the data needed, and completing and reviewing the collection of information. Send comments regarding this burden estimate or any other aspect of this collection of information, including suggestions for reducing this burden, to Washington Headquarters Services, Directorate for Information Operations and Reports, 1215 Jefferson Davis Highway, Suite 1204, Arlington VA 22202-4302. Respondents should be aware that notwithstanding any other provision of law, no person shall be subject to a penalty for failing to comply with a collection of information if it does not display a currently valid OMB control number.

| | | | | | |
|------------------------------------------------------------------------------------------------------------------------------------|------------------------------------|-------------------------------------|----------------------------|-----------------------------------------------------|---------------------------------|
| 1. REPORT DATE 30 SEP 2006 | | 2. REPORT TYPE | | 3. DATES COVERED 00-00-2006 to 00-00-2006 | |
| 4. TITLE AND SUBTITLE High Frequency Acoustic Channel Characterization for Propagation and Ambient Noise | | | | 5a. CONTRACT NUMBER | |
| | | | | 5b. GRANT NUMBER | |
| | | | | 5c. PROGRAM ELEMENT NUMBER | |
| 6. AUTHOR(S) | | | | 5d. PROJECT NUMBER | |
| | | | | 5e. TASK NUMBER | |
| | | | | 5f. WORK UNIT NUMBER | |
| 7. PERFORMING ORGANIZATION NAME(S) AND ADDRESS(ES) HLS Research Inc,12730 High Bluff Drive, Suite 130,San Diego,CA,92130 | | | | 8. PERFORMING ORGANIZATION REPORT NUMBER | |
| 9. SPONSORING/MONITORING AGENCY NAME(S) AND ADDRESS(ES) | | | | 10. SPONSOR/MONITOR'S ACRONYM(S) | |
| | | | | 11. SPONSOR/MONITOR'S REPORT NUMBER(S) | |
| 12. DISTRIBUTION/AVAILABILITY STATEMENT Approved for public release; distribution unlimited | | | | | |
| 13. SUPPLEMENTARY NOTES | | | | | |
| 14. ABSTRACT | | | | | |
| 15. SUBJECT TERMS | | | | | |
| 16. SECURITY CLASSIFICATION OF: | | | 17. LIMITATION OF ABSTRACT | 18. NUMBER OF PAGES | 19a. NAME OF RESPONSIBLE PERSON |
| a. REPORT unclassified | b. ABSTRACT unclassified | c. THIS PAGE unclassified | | | |

autonomous system developed at the University of Algarve, Portugal. The AOB2 is a drifting 8-element self-recording array that resembles the size and weight of a standard sonobuoy. The operating area is shown in the left panel of Fig. 1 where the bathymetry is color coded (bathymetry survey was conducted by the University of New Hampshire Center for Coastal and Ocean Mapping). The right panel in Fig. 1 shows the experimental geometry and water depths at the equipment locations. Figure 2 shows the configuration of the AOB2 receiving array and a picture of the deployed buoy.

Modeling approach

The modeling approach used is based on the Gaussian Beam Tracing code implemented in Bellhop [Porter and Bucker]. From Bellhop, for each source-receiver pair, N arrival amplitudes, $A_n(\omega)$, and delays, $\tau_n(\omega)$, are calculated. The pressure field, $p(t)$, can be represented as a sum over arrivals according to,

$$p(t) = \sum_{n=1}^N \text{Re}\{A_n(t)\}s(t - \tau_n) - \text{Im}\{A_n(t)\}s^+(t - \tau_n) \quad (1)$$

where s^+ is the Hilbert transform of the source function $s(t)$. The Hilbert transform is a 90° phase shift of $s(t)$ and accounts for the imaginary part of A_n . Equation (1) can be interpreted as saying that any arbitrary phase change can be understood as a weighted sum of the original waveform and its 90° phase-shifted version. The weighting controls the effective phase shift.

A straight application of Eq. (1) requires computing the amplitudes and delays on an incredibly fine spatial grid since the amplitudes are needed for each time step. This degree of spatial sampling is not very practical; however, using a Gaussian Beam approach allows for spatial interpolation and extrapolation of arrival amplitudes and delays. This is possible since arrival patterns vary slowly over spatial scales of several to hundreds of wavelengths. One difficulty often encountered with arrival interpolation is the so-called ray identification problem. That is, to calculate the field between grid points, the same arrival type (i.e. direct path, surface bounce etc.) needs to be identified before interpolating its amplitude and phase. This sounds simple enough but can be problematic since arrivals on one grid point may not correspond to those at another. That is, reflection and refraction can cause both a different number of rays and different ray-types on each of the grid points. For example, consider the direct path on one grid point that is refracted away from another grid point. In this case, interpolating the first arrival between these grid points may involve interpolation of a direct path with a bottom-bounce path and this will produce incorrect results. This problem can be avoided without keeping track of arrival types by using an approach similar to using shape functions in finite-element methods. The influence of these shape functions can be computed independently but their sum provides the equivalent of a bilinear interpolation. Consider a rectangular grid with receiver location somewhere in the middle of four grid points. The amplitudes at the grid points are maintained as separate quantities and their corresponding delays are adjusted by the ray path travel-time differences between the grid point and the receiver location. The amplitudes are adjusted by the appropriate travel distance. The received field is constructed using Eq. (1) with an additional sum over each of the arrivals on the four grid points. The weight given to each grid point is based on bi-linear interpolation. The arrivals are never interpolated between grid points, therefore, sorting and interpolating based on arrival types is not necessary and results are surprisingly good.

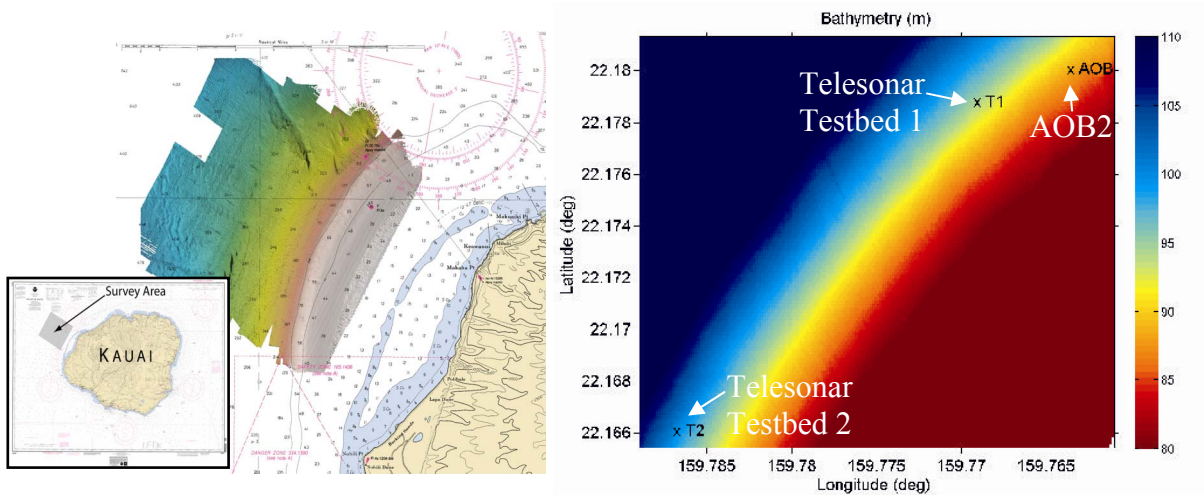


Figure 1: Makai 2005-Left panel shows the bathymetry survey area relative to Kauai, HI (survey was made by University of New Hampshire, Center for Coastal and Ocean Mapping). Right panel shows the configuration and water depth of the September 24, 2005 experiment. The AOB2 was free drifting, Telesonar Testbed 2 was moored and Testbed 1 was towed from R/V KiloMoana.

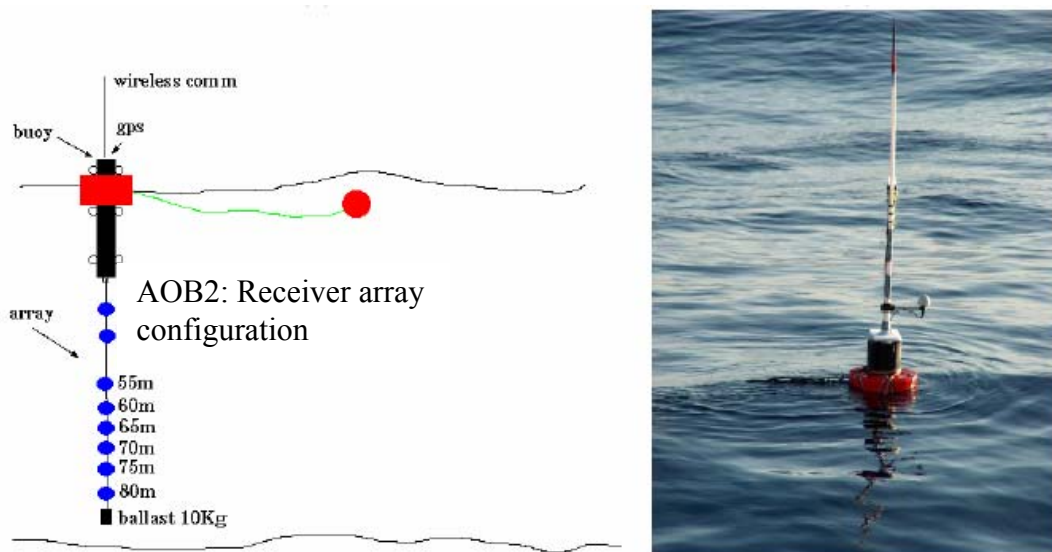


Figure 2: Makai 2005- Left panel shows the configuration of the receiver elements in the AOB2 buoy (developed by the University of Algarve, Portugal). Right panel shows the deployed buoy.

Simple surface motion (i.e. slowly changing in time and space) can be treated in this manner by extending the interpolation. This adds another dimension and results in the sum of arrivals being calculated on eight grid points. This simple model was sufficient to explain the Makai observations but initial research was also done on a more sophisticated time-domain surface scatter model. The Helmholtz integral equation was used with the Kirchhoff approximation. The Green's functions representing the impulse response from all scattering points on the surface to the receivers was computed in terms of arrival amplitudes and time delays. This time-domain framework allows for including both broadband signals and a realistic, time-varying sea-surface. The method was compared with exact solutions for a sub-set of problems (frozen, rough surfaces) to determine limitations [3].

WORK COMPLETED

Measurements and Modeling of Doppler Sensitive Waveforms

The Makai 2005 data were modeled using a dynamic sea-surface and moving receiver array as previously described. This was done for both stationary and moving platforms at various source-receiver ranges. The important Doppler effects that were observed in the data were adequately modeled [4,5].

Adaptive beamforming of ambient noise

Adaptive beamforming methods (i.e. Minimum Variance Distortionless Processor) were applied to data sets collected in the Mediterranean Sea. The improved resolution allowed better identification of the seabed layering. This layering information was included in a geoacoustic inversion scheme to determine the sound speed, density and attenuation of each layer [2].

RESULTS

Model-Data comparisons of Doppler Sensitive Waveforms

The transmission shown here is from the towed Testbed T1 and was received on the AOB2 about 600 m away (JD 268 at 01:02). Modeled and measured receptions on the deepest 6 hydrophones of the AOB are shown in Fig. 3. A 0.7 second BPSK (binary-phase-shift-keying) transmission was used for the analysis. This waveform is commonly used for communications but for this analysis is simply a highly Doppler-sensitive signal. The transmission used cycles of a 9.5 kHz sinusoid with phase shifts introduced to represent a string of 1's and 0's defined by an m-sequence. In a static situation, using a matched filter on this waveform produces an estimate of the channel impulse response. However, in situations with source/receiver motion, each path can have a different Doppler shift (due to the angle-dependent propagation paths). A Doppler shift can be applied to the BPSK transmit signal before the matched filter process. By sweeping over a variety of shifts, the Doppler for each received arrival can be estimated. In Fig. 3, the data are matched-filtered using different Doppler corrections and the maximum value for each arrival is taken in the plot. This type of figure provides a check of the experiment geometry and matched filter process. The arrivals in Fig. 3 correspond to different acoustic paths which can be seen using a ray trace diagram (as in panel (c) of Fig. 4).

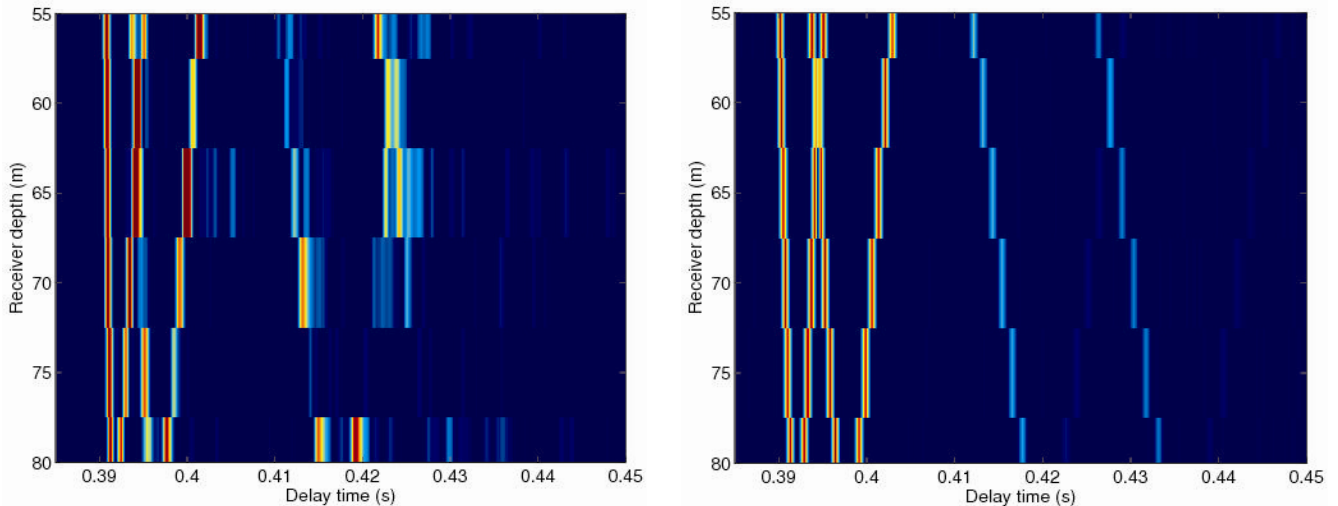


Figure 3: Left panel: impulse response on the AOB2 array with optimal Doppler correction for each path. Delay times for arrivals are shown along the x-axis for various depths (y-axis). Right panel: modeled (static) impulse response for the assumed geometry.

An important quantity for communications is the Doppler spread, which depends on how the various acoustic paths are Doppler shifted. A convenient way to present this information is with the so-called channel “scattering function”. In Fig. 4, receptions are shown from Testbed 1 to a single channel on the AOB2. The bright spots indicate an arrival in time along the x-axis while the y-axis indicates the amount of Doppler introduced. The y-axis shows the relative speed that corresponds to the peaks. Doppler indicates the relative speed between the AOB2 and Testbed 1 was about 1.2—1.4 m/s (estimate from GPS positions indicated about 1.24 m/s). The first arrivals show decreasing Doppler for the first few arrivals followed by the last arrivals having increased Doppler shift. For horizontal velocity one expects the later arrivals to have decreasing Doppler shifts due to higher propagation angles relative to the direction of motion. The high Doppler on the last arrivals implies a component in the vertical velocity which would introduce larger shifts for late arrivals. It is critical to correctly identify the paths so that the proper Doppler mechanism is attributed. That is, Doppler associated with the bottom bounce path can be attributed to receiver motion but not to surface motion, while a surface bounce path can have Doppler contributions from both. In panel (c) of Fig. 4, a ray trace of the geometry is shown and the paths are numbered corresponding to (1) direct, (2) surface bounce (3) bottom bounce (4) surface-bottom bounce and (5) bottom-surface bounce. These paths are also labeled on the measured arrivals shown in panel (a). The different path directions have sensitivity to different velocity components. The higher numbered paths are more Doppler sensitive to the vertical velocity components and the lower numbered paths (e.g. direct path) are more sensitive to the horizontal velocity components. In panel (a) note that the surface-bottom arrival has a positive Doppler shift relative to the direct path and the bottom-surface has a negative shift. In panel (b) of Fig. 4 the model results are shown. To correctly model the Doppler on each path the sea-surface motion required motion in different directions depending on the arrival.

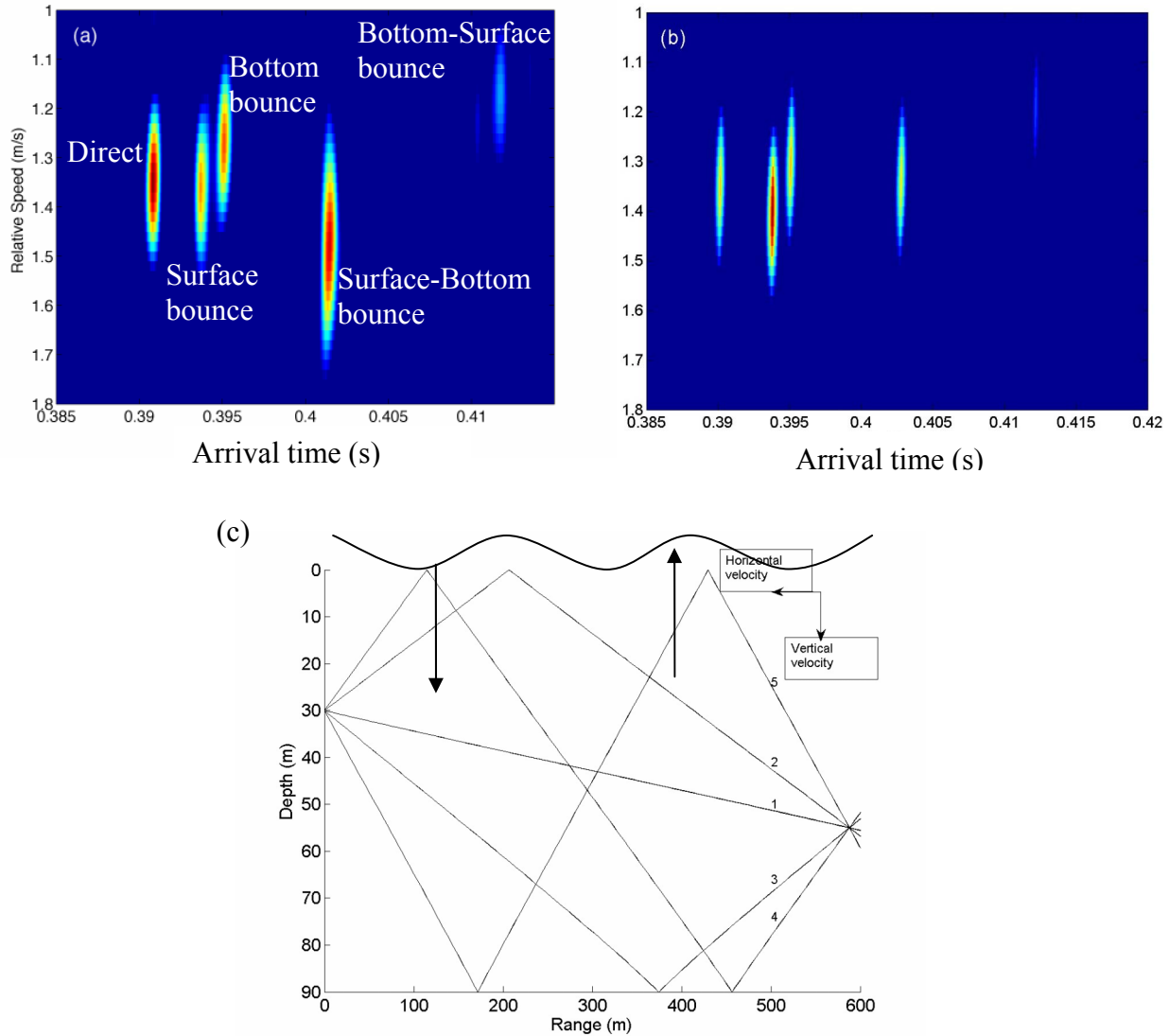


Figure 4: Panel (a) shows the measured impulse response for various Doppler shifts (in terms of relative speed) indicated on the y-axis between the drifting AOB2 and the towed TB1 source. The horizontal axis is delay time in seconds. Each bright spot is an arrival. In panel (b) is the modeled result using a simple moving sea-surface that allows different paths to experience different motion from the sea-surface. In panel (c) is the ray trace diagram. The arrivals are numbered (1) direct path, (2) surface bounce, (3) bottom bounce, (4) surface-bottom bounce and (5) bottom-surface bounce. The steeper paths are more sensitive to vertical velocity components (e.g. from the surface) than the horizontal paths.

Results from adaptive beamforming of ambient noise data

Recent results have shown that the ambient noise field can be processed to produce reflections from the seabed and sub-bottom layering [1,2]. These passive processing results are similar to those obtained using active systems such as a chirp-sonar. Improved processing results were obtained using adaptive processing methods (i.e. Minimum Variance Distortionless Processor). In Fig. 5, results are shown from data processed both with conventional and adaptive methods. In both cases the seabed reflection is quite strong and evident. However, the adaptive results show better resolution and an enhancement in the reflections from deeper layers.

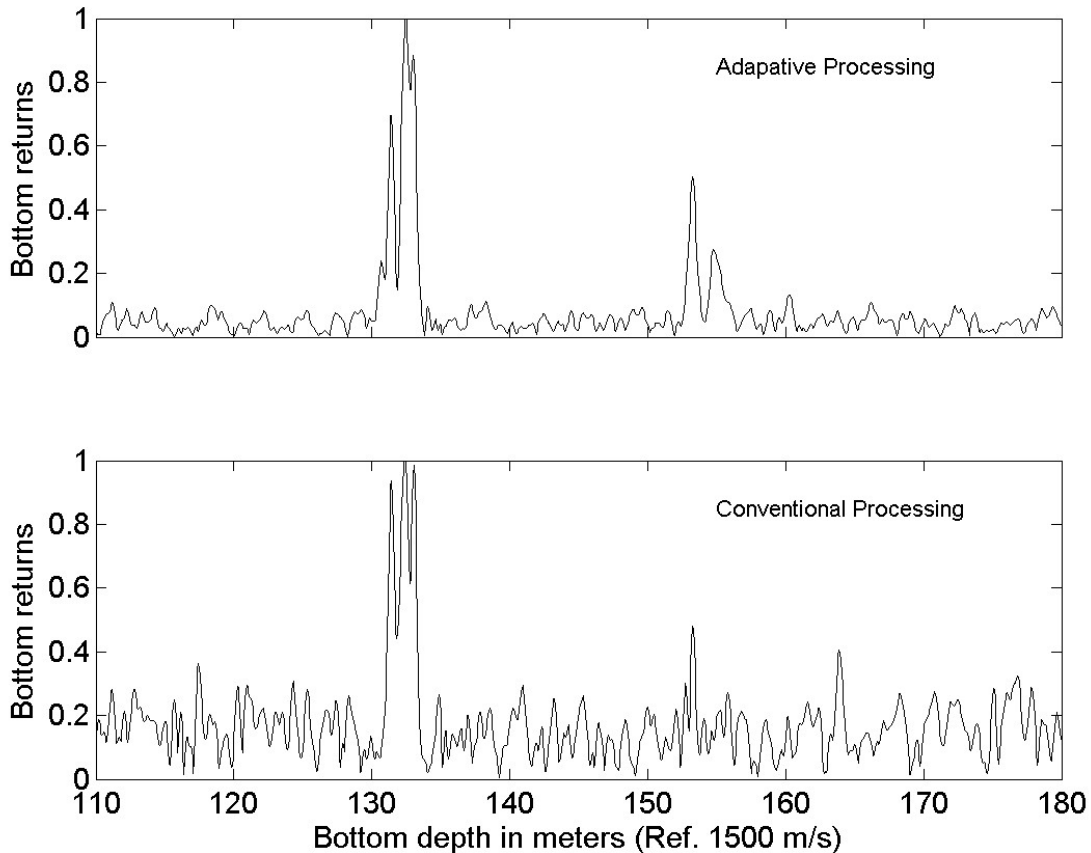


Figure 5: Top panel shows the bottom returns obtained from ambient noise using adaptive processing. The lower panel is the same data using conventional processing. The adaptive method gives a better indication of the layering.

IMPACT/APPLICATIONS

This work has the potential for significant impact on several sonar systems and underwater acoustics applications (e.g., ASW, MCM, underwater acoustic communications). In particular, the acoustic communications modeling is leading to improvements in predicting system failures and ways to better deploy modems. The ambient noise work is progressing towards an efficient and practical way to identify the seabed properties. This will have a significant impact on sonar performance and predicting

TRANSITIONS

A new 6.4 project under Intelligence, Surveillance, Reconnaissance, and Information Operations (PMW 180) is planned for FY07 and will use the work developed under this ONR project on ambient noise processing to estimate seabed properties. These techniques will transition through the Navy Oceanographic Office. A prototype system is planned for development in FY07.

RELATED PROJECTS

This research has been done in collaboration with Michael Porter and the ONR High Frequency Initiative and the ONR PLUSNet program.

REFERENCES

M. B. Porter and H. P. Bucker, "Gaussian beam tracing for computing ocean acoustic fields," *J. Acoust. Soc. Am.* **82**, (4), 1349–1359 (1987).

PUBLICATIONS

[1] Martin Siderius, Chris Harrison and Michael Porter, "A passive fathometer for determining bottom depth and imaging seabed layering using ambient noise", *J. Acoust. Soc. Am.*, **120** (3), pp. 1315-1323, (September, 2006).

[2] Martin Siderius, Michael B. Porter and Chris Harrison, "Recent developments in ambient noise processing (A)", (Invited), *J. Acoust. So. Am.* **119**, 3217 (June,2006).

[3] Martin Siderius, Michael B. Porter, and Ahmad T. Abawi, "A time domain approach to sea-surface scattering (A)", *J. Acoust. Soc. Am.* **119**, 3217 (June, 2006).

[4] Martin Siderius, Michael B. Porter, Paul Hursky, and Vincent McDonald, "Modeling Doppler effects for acoustic communications (A)", *J. Acoust. Soc. Am.* **119**, 3217 (June, 2006).

[5] Martin Siderius, Michael B. Porter, Paul Hursky and Vincent McDonald, "Modeling Doppler Sensitive Waveforms Measured off the Coast of Kauai", *Proceedings of the Eighth European Conference on Underwater Acoustics*, Eds. S. M. Jesus and O. C. Rodriguez, (June, 2006).

[6] Chris H. Harrison and Martin Siderius, "Using Beam-Beam Cross-Correlation of Noise to Investigate Back-Scatter", *Proceedings of the Eighth European Conference on Underwater Acoustics*, Eds. S. M. Jesus and O. C. Rodriguez, (June, 2006).